This preprint was submitted to Aquatic Sciences for peer review and publication
(Twitter: @shubhamrockz_05, @ulloa_hn)

Disentangling the effects of climate change and reoligotrophication on primary production in a large lake

Shubham Krishna[1,3], Hugo N. Ulloa[2,3], Emile Barbe[3] and Alfred Wüest[3,4]

Received: date / Accepted: date

Abstract Climate change and reduction in nutrient loads have significant effects on primary production and phytoplankton growth dynamics. Since in the last few decades in many regions, nutrients in lakes were reduced simultaneously as the climate changed. Yet, it remains unclear which of the two has impacted primary production the most. In this study, we couple the General Ocean Turbulence Model with the Ecological Regional Ocean Model to disentangle the effects of climate change and reoligotrophication on primary production (PP) in Lake Geneva, Switzerland-France. We apply a data assimilation method to calibrate the model with the observations from the past (1981-1990) and validate it against the in-situ data from the present decade (2011-2019). Both decades represent different climate conditions and trophic states of the lake. We show that the model is skilful to reproduce assimilated and unassimilated observations from both periods. According to our results, the effect of reoligotrophication on PP is marginally higher than that of warming, leading to a net decrease in primary production by 10% from the past to the present. The areal phosphorus supply in Lake Geneva, in spite of a decrease by ~70%, is still characteristic of a meso-to-eutrophic ecosystem. This points towards an incomplete reoligotrophication of the lake. The effects of future climate change on winter mixing and PP dynamics have also been studied. Although there would be a significant reduction in deep mixing, the autotrophic production in Lake Geneva is expected to increase by ~20% by the end of 21st century, largely due to stimulation in biomass build-up of temperature-dependent algae (e.g. dinoflagellates and cyanobacteria). Considering our results to represent other large temperate lakes with similar trophic status and water residence time as Lake Geneva, future climate scenarios are expected to bring back symptoms of eutrophication.

Keywords Warming · eutrophication · oligotrophication · global-warming · carbon-fixation · phytoplankton · mixing · trophic-status · nutrient-supply

1 Introduction

Lakes are sentinels of climate change and increasing anthropogenic pressures (Adrian et al. 2009). The imprints of alteration in the dynamics of physical and biogeochemical processes are visible in long-term records but also in the monitoring of limnic indicators in rather short periods. By studying the long-term changes in the key parameters such as water temperature, transparency, turbidity, primary production (PP) and nutrient concentrations, the impact of stressors can be assessed. Besides being scientifically relevant, lakes have significant socio-economic values. They are an essential source of drinking water, contain large stocks of marketable fish, and attract tourists for leisure activities. However, all the values mentioned above are linked to the health of the lake ecosystem, greatly affected by global warming and

Shubham Krishna
E-mail: shubham.krishna@hereon.de

Hugo N. Ulloa
E-mail: ulloa@sas.upenn.edu

Emile Barbe
E-mail: emile.barbe@alumni.epfl.ch

Alfred Wüest
E-mail: Alfred.Wueest@eawag.ch

[1] Helmholtz-Zentrum Hereon GmbH, Max-Planck-str. 1, 21502 Geesthacht, Germany
[2]Department of Earth and Environmental Science, University of Pennsylvania, Philadelphia, PA, USA
[3] Limnology Center, École Polytechnique Fédérale de Lausanne, CH-1015 Lausanne, Switzerland
[4] Eawag, Swiss Federal Institute of Aquatic Science and Technology, Department of Surface Waters – Research and Management, Seestrasse 79, CH-6047 Kastanienbaum, Switzerland

eutrophication (Adrian et al. 2009; Williamson et al. 2009; Schindler 2009).

Over the past few decades, lakes around the world have been exposed to both eutrophication and climate change that are known to have synergistic effects on the food web dynamics (Moss et al. 2011). Eutrophication poses a severe threat to freshwater ecosystems as it leads to significant changes in the food web structure, water quality and hypoxic conditions (Hecky 1993; Carpenter et al. 1999). In Europe, eutrophication was a big concern as recent as the end of the 20th century, and it is still the case for lowland and subalpine lakes (Anderson et al. 2014). However, eutrophication remains being a serious challenge and increasing in many regions around the globe, pervasively degrading the quality of lakes. To mitigate eutrophication, significant regulatory efforts were taken to reduce nutrient inputs to lakes (Schindler et al. 2016). Especially phosphorus (P) loads, as it is considered the critical limiting nutrient for phytoplankton growth and PP in lakes. The recent reversal in the trophic status is commonly referred as reoligotrophication (Edmondson and Lehman 1981). As a consequence of the decline in external loadings, lakes in Western Europe, particularly in the alpine region, started to transition from eutrophic to mesotrophic and partly even to oligotrophic states (Müller et al. 2019). Interestingly, despite massive reductions in nutrient loads, PP in these lakes did not decrease as expected (Finger et al. 2013; Lepori et al. 2018; Anneville et al. 2019). Different hypotheses have been suggested for the resistance of PP against decline, such as the impact of climate change being higher than reoligotrophication, lower grazing pressure and an increase of the nutrient recycling rate. It is to note that full mixing events rarely happen in the large alpine lakes (such as Lake Geneva), and therefore internal loadings (nutrients released by the sediments) do not directly support pelagic PP. Instead, it is the strength of winter convection that controls PP by supplying regenerated nutrients from hypolimnion (Schwefel et al. 2016; Krishna et al. 2021).

Along with eutrophication, climate change has also affected dynamics of lakes worldwide (O'Reilly et al. 2003; Lepori and Roberts 2015; Woolway et al. 2017). Consistent warming over the last four decades has led to longer and stronger stratified periods, weaker seasonal deep mixing, and proliferation of harmful algae in freshwater bodies (Schindler 1997). For temperate lakes, the reduction in nutrient loads happened often simultaneously as global warming. The concomitant effect of these two drivers on PP is complex. While reoligotrophication should contribute to a decline in PP, climate warming driven stimulation in remineralization rates of organic matter and intensification of cyanobacterial blooms have a positive effect on autotrophic production. Therefore, to investigate the long-term changes in PP in limnic ecosystems, it is important to disentangle the effects of climate change and reoligotrophication and study their synergistic controls on phytoplankton growth dynamics (Anderson et al. 2005; Tirok and Gaedke 2007; Moss et al. 2011; Finger et al. 2013).

Although the observations on PP and chlorophyll concentrations provide monitoring of changes in the trophic state of lakes, it is hard to quantify the effects of individual drivers on PP from in-situ data. Ecological models are widely utilized to study PP and phytoplankton growth (Kerimoglu et al. 2017; Ward et al. 2020; Krishna et al. 2021), physiology of planktonic community (Elliott et al. 2006; Rinke et al. 2009), the ecosystem response to past, present and future climate forcing (Straile et al. 2010; Wilson et al. 2018; Gray et al. 2019; Farrell et al. 2020) and to reduction in nutrient loads for lake management purposes (Reynolds 1999; Trolle et al. 2008; Lindim et al. 2015). Furthermore, by applying mechanistic models, it is possible to investigate the second-order synergistic effects of reoligotrophication and climate change on PP.

Lake Geneva is a sub-alpine lake that has undergone a significant reduction in nutrient loads while experiencing warming (Tadonléké et al. 2009; Schwefel et al. 2019). However, the PP patterns remain variable, and no long-term trend could be identified. In this study, a coupled physical-biogeochemical model, GOTM-ERGOM, was set up to simulate long-term PP and nutrient dynamics in Lake Geneva from the past and present periods, 1981 to 1990 (P1) and 2011 to 2019 (P2), respectively. We calibrate the model with the observations from P1 and validate against those from P2. In this manuscript, we report two distinct analyses. Firstly, we focus on disentangling and quantifying the effects of climate change and reoligotrophication on PP. Secondly, we investigate the effects of future climate change scenarios on PP. Thus, from our results, we seek to (1) understand how PP dynamics in Lake Geneva respond to changes in external nutrient loading and warming and (2) shed light on the lake future trophic pathway.

2 Materials and methods

2.1 Study site

Lake Geneva, the largest freshwater body in Western Europe (580 km^2 and 89 km^3), is located between France and Switzerland (46.45° N, 6.52° E) at an altitude of 372 m. It is a deep peri-alpine lake, with an average depth of 153 and a maximum of 309 m. The Rhône River is by far its main tributary, as it accounts for about 75% of the total inflow. The water residence time in Lake Geneva is about 11.3 years. Lake Geneva is a monomictic lake that remains thermally stratified from spring to autumn (Schwefel et al. 2016). The watershed of Lake Geneva saw intense urbanization and industrialization between 1960 and 1980. Consequently, the total phosphorus (TP) concentrations in the lake rose from 10 to 90 $\mu gP\ L^{-1}$. In response to the potential threats posed by the highly eutrophic state of the lake, the Governments

of France and Switzerland founded the International Commission for the Protection of Lake Geneva (CIPEL). The main objective of CIPEL was to propose and to monitor coherent measures to reduce phosphorus loads to Lake Geneva significantly, which turned out to be successful as TP levels dropped down to ~20 μgP L^{-1} (present-day).

2.2 Meteorological forcing and in-situ measurements

The meteorological forcing used in this study are obtained from two sources. For the P2 (2011-2019) simulation, the hourly solar radiation, air temperature, atmospheric pressure, relative humidity and cloud cover data are extracted from the Consortium for Small-scale Modelling (COSMO) simulations (Baldauf et al. 2011). The advantage of using COSMO data is its high spatial resolution, which is 1.1 km. Unfortunately, this dataset is available only since 2007. For the P1 (1981-1990) simulation, we derived the meteorological forcing from the European Centre for Medium Range Weather Forecasts (ECMWF) System (Molteni et al. 1996). For both the periods, the model is forced with hourly meteorological data, except the precipitation data which is available at daily-average resolution.

Lake Geneva has a long monitoring history. In-situ measurements of physical and biogeochemical parameters (e.g. water temperature, nutrients, PP, and dissolved oxygen profiles) are available from three monitoring stations (SHL1, SHL2, GE3) in the lake (Rimet et al. 2020). The SHL2 monitoring station (46.45° N, 6.59° E), located at the deepest point of the lake, has the longest uninterrupted time series of measurements. Samples are collected once per month in winter and twice per month during the productive season (March-November). Figure 1 shows the long-term series of the measured temperature, dissolved inorganic phosphorus (DIP) and dissolved inorganic nitrogen (DIN) concentrations, and dissolved oxygen (DO) from P1 and P2 for the top 20 m of the lake. In-situ data show that the upper water column of the lake has already warmed by 1.5°C over the last four decades. Furthermore, during this period, a significant reduction in DIP concentrations (from 2.5 mmol P m^{-3} to 0.5 mmol P m^{-3}) took place. However, there is no significant change in DIN concentrations.

2.3 Annual phosphorus budget

The annual phosphorus uptake in the productive layer (P-uptake) to sustain PP is calculated from the annual P-budget, given by the difference of the source and sink terms of P load (Krishna et al. 2021; Steinsberger et al. 2021). The source terms include the watershed contributions of the bioavailable dissolved reactive phosphorus (from the rivers and wastewater treatment plants around Lake Geneva), represented as $\mathcal{DRP}_{in}$, and the net difference of P stock in the epilimnion before and after the production period (Fig. 2), which is from March to October and most of the annual primary production happens during this time. Whereas the riverine output load ($\mathcal{TP}_{out}$) and the annual sedimentation load ($\mathcal{TP}_{sed}$) account for the sink terms. Thus, the P-uptake is determined by the following budget:

$$P_{uptake} = \mathcal{DRP}_{in} - \mathcal{TP}_{out} - \mathcal{TP}_{sed} + \int_0^{z_{epi}} A(z)\,[TP]_{mix}\,(z)\,\mathrm{dz} - \int_0^{z_{epi}} A(z)[TP]_{aut}\,(z)\,\mathrm{dz}\,. \tag{1}$$

Every term in (1) has units of tons year^{-1}. The term '$\int_0^{z_{epi}} A(z)\,[TP]_{mix}\,(z)\,\mathrm{dz} - \int_0^{z_{epi}} A(z)[TP]_{aut}\,(z)\,\mathrm{dz}$' is the difference in the TP stock in the epilimnion over the productive period in the trophogenic layer, where $[TP]_{mix}$ is the TP load in the productive layer, after winter mixing, in March and $[TP]_{aut}$ is the TP load left after the productive period in October. The productive layer was defined between 0 and z_{epi} = 20 m based on the analysis of long-term phytoplankton biomass concentration and PP profiles (not shown here, Tadonléké et al. 2009). The area as a function of depth, $A(z)$, was taken from hypsometric curves (Federal Office of Topography, 2017). $\mathcal{DRP}_{in}$ and $\mathcal{TP}_{out}$ are computed from the watershed data (Müller et al. 2019). Steinsberger et al. (2021) estimated a consistent value of 11.3 gC m^{-2} for the annual net sedimentation (NS) in Lake Geneva using long-term data and previous sediment core measurements. We apply annual P:C ratios (of seston) to NS to compute $\mathcal{TP}_{sed}$ for the years in P1 and P2.

2.4 Model description

We use the Framework of Aquatic Biogeochemical Models interface (Bruggeman and Bolding 2014) to couple GOTM with ERGOM. GOTM is a one-dimensional, physical, water column model that describes vertical turbulent fluxes of momentum, temperature, and salinity (Burchard et al. 2006). Turbulence and tracer transport are modelled by Reynolds-averaged Navier–Stokes (RANS) equations in a rotating reference frame. A detailed description of GOTM is provided in Burchard et al. (2006). For Lake Geneva, we use GOTM-lake, a branch of GOTM designed for freshwater ecosystems. The depth of water column to be simulated is prescribed in "gotmrun.nml" file. It is 309 m for Lake Geneva. The number of depth levels are given by *nlev* parameter in the same file. We choose 200 depth levels, based on our previous study (Krishna et al. 2021). By adjusting the grid zooming parameters, *ddu* and *ddl*, it is possible to increase the spatial resolution (higher number of levels) towards the surface or the bottom. In our setup, we have higher resolution for the lake epilimnion. GOTM-lake considers a hypsography file which lists the surface area of the lake covered by each discrete

depth contours. The deeper waters of Lake Geneva have smaller surface area and this information is passed on to the model by the hypsography file. Thus, it avoids the problem of overestimating the winter mixing, which was the case with the older version of GOTM. For more details on GOTM-lake model, we suggest referring to Chen et al. (2019) and Wilson et al. (2020).

ERGOM is a medium-complexity ecological model, originally developed to resolve ecosystem dynamics of the Baltic Sea (Neumann 2000). However, it has been also applied to study freshwater food webs (Darko et al. 2019; Krishna et al. 2021). The model consists of 10 state variables and is based on a Nutrients, Phytoplankton Zooplankton, and Detritus (NPZD) framework. The nutrient state variables are dissolved inorganic nitrate, dissolved ammonium and DIP. The phytoplankton compartment is represented by three functional groups: diatoms, flagellates, and cyanobacteria. Diatoms are assumed to grow in nutrient-rich conditions and are limited by DIN and DIP. The growth rate of flagellates depends on DIN and DIP concentrations and water temperature. Cyanobacteria are limited only by DIP, and their growth rates have strong temperature dependence and are assumed to survive in low nutrient conditions (typical in summer). In the model, all three types of phytoplankton are grazed by zooplankton. However, the affinity for cyanobacteria is lower compared to diatoms and flagellates. The dead phytoplankton and zooplankton become part of detritus. A fraction of the detritus mineralizes into DIN and DIP which is temperature-dependent, while the rest reaches the bottom layer represented by the sediment compartment. Oxygen dynamics in the model depend on PP, remineralization, nitrification, and denitrification processes. The detailed description of ERGOM equations is given in Neumann et al. (2002) and Krishna et al. (2021).

2.5 Data assimilation method: model calibration and parameter uncertainty estimation

We calibrate the model with the observations from the past decade, P1, and validate it against in-situ data from the present decade (P2). Both periods (P1 and P2) represent distinct trophic status and climate regimes. P1 represents the eutrophic state of the lake, and P2 is marked by eu- to mesotrophic conditions and warmer water. We designed a data-model misfit function (cost function, denoted by J), which is minimized by the 'Broyden–Fletcher–Goldfarb–Shanno' (BFGS) optimization algorithm (Dennis Jr and Schnabel 1996) to yield the optimized set of parameters for P1. This simulation represents high nutrients and low air temperature scenario, and hence we call it $H_N L_T$. Two measured variables (DIP, PP) are assimilated in the cost function. We assess the model's robustness by simulating P2 (low nutrients and high air temperature condition) with the optimized solution of P1, and this run is termed as $L_N H_T$. The definition of the cost function is given below:

$$J = \frac{\sum_{i=t_1}^{t_n} (obs_i - mod_i)^2}{\sigma_{obs}^2}, \tag{2}$$

where obs_i and mod_i are the annual averages of the observed and modelled variables, and σ_{obs}^2 is the variance over the decade. The design of the cost function is similar to that of Schartau and Oschlies (2003) and of Krishna et al. (2021).

We selected five ecological parameters for the optimization procedure: the maximum potential growth rates of diatom, dinoflagellates and cyanobacteria (r_1^{max}, r_2^{max} and r_3^{max}), the maximum grazing rate (g_{max}), and the remineralization rate (l_{da}), for the optimization procedure. The selection of these parameters is based on a prior sensitivity analysis (not shown here) and on their relevance for PP in Lake Geneva (Krishna et al. 2021). The rest of the model parameters were prescribed fixed values adopted from Krishna et al. (2021), see Table 2. The model parameter representing P:N ratio of seston (rfr) was adjusted according to the lake's trophic state. It has been shown that P:N of lake seston changes with nutrient concentrations (Van Donk et al. 2008). For eutrophic lakes, this ratio is above 0.04, and for mesotrophic conditions it is below 0.03 (Forsberg and Ryding 1980). Hence, we assumed $rfr = 0.05$ for P1 and $rfr = 0.03$ for P2 (Table 3). These values are comparable to the observed P:N ratio of seston in Lake Geneva (Steinsberger et al. 2021).

To estimate the parameter uncertainties, we applied modMCMC function available in the FME package that performs Markov chain Monte Carlo (MCMC) simulations. The algorithm yields an ensemble of model solutions that corresponds to uncertainties associated with the optimized parameter values.

2.6 Model simulations and scenarios

In addition to the $H_N L_T$ and $L_N H_T$ simulations, we perform two more model runs with different combinations of the trophic states and climate conditions (Fig. 3) to disentangle the effects of climate change and reoligotrophication on PP. The extreme case considers the present climate and eutrophic condition denoted as $H_N H_T$. This case is simulated by forcing the $L_N H_T$ solution with the external nutrient loadings of P1. Likewise, for the $L_N L_T$ simulation, which represents the low nutrients and low-temperature conditions, the $H_N L_T$ setup is perturbed with the nutrient levels of P2. As indicated earlier, for all the simulations, we force the model by hourly input data and we integrate numerically the governing equation with a time step of one hour. Table 1 summarises ERGOM's state variables for scenarios P1 and P2.

In order to study the response of the ecosystem to future climate change, meteorological forcing data are prepared based on the representative concentration pathway (RCP) scenarios set by the Intergovernmental Panel on Climate Change (IPCC 2014). The Swiss National Center for Climate Services (NCCS) determined the ranges for the seasonal changes in air temperature and solar radiation by the end of the 21st century (from year 2085 to 2090) for the regions in Switzerland. These changes are expressed relative to the present period. The median values of these seasonal changes, corresponding to the RCP8.5 scenario, were taken and directly added to the air temperature and radiation time series for the 2014-2019 period. To simulate the future scenario, the model is forced with this climatological Data.

3 Results

We calibrated the ecological model with the observed annual PP and DIP from the past period (P1) and validated it against the observations (water temperature, DIN, P-uptake, DO) that were not assimilated in the cost function for the periods P1 and P2. To quantify and assess the model skills, we computed and analysed the root mean squared errors (RMSEs) and mean absolute errors (MAEs). From our data assimilation approach, we obtain the uncertainties associated with parameter estimates and the optimized ("best") model solution which yields the lowest misfits in the simulated and observed PP and DIP for P1. The optimized estimates of the parameters are listed in Table 4. The model predicts the values 1.3, 0.9 and 0.4 d^{-1} for r_1^{max}, r_2^{max}, and r_3^{max}, respectively, which are comparable to those identified in other modelling studies (Neumann 2000; Neumann et al. 2002; Krishna et al. 2021). We applied the MCMC method to estimate the parameter uncertainties that originate from structural deficiencies in the model and uncertainty in the observations (Schartau et al. 2017). In spite the low resolution observations, four out of five parameters are well constrained and yield low uncertainties. This highlights the robustness of the model. The lowest uncertainties are predicted for the growth rate parameters, r_1^{max}, r_2^{max}, and r_3^{max}, that correspond to variations between 5% to 10% from the optimized solution. The largest uncertainty is obtained in the estimate of l_{da}, around 100% variation from the optimized value (Table 4). Typically, the degradation rates of organic matter in lakes show high seasonality and are highly dynamic temporally, especially in epilimnion and metalimnion. The large uncertainty in l_{da} could result from the fact that we assimilate annual average observations in our misfit function which masks the seasonality signal, and hence it becomes difficult to constrain the parameter. In addition, the lack of suitable observations, e.g. Particulate Organic Matter (POM) and detritus concentration, also contributes to the uncertainty.

3.1 Model calibration and validation

The physical model reproduces well the observed temperature patterns in the productive layer for P1 and P2 (Fig. 1). It yields RMSE and MAE values of 0.70°C and 0.40°C in P1 and 0.61°C and 0.35°C in P2 (Tables 5 and 6). The misfits between the model and observations are slightly higher in P1 compared to P2, but well within the usual deviations of 1-dimensional models. Notice that the P2 simulation may have lower uncertainties than the P1 simulation. The latter is most likely because the meteorological forcing derived from COSMO data has a higher spatial resolution and provides more reliable weather conditions at the SHL2 station (the long-term monitoring point in Lake Geneva) than ECMWF data.

The optimized solution for P1 predicts the annual-averaged PP (top 30 m) with RMSE of 6.70 gC m^{-3} and MAE of 6.10 gC m^{-3} and yields RMSE of 0.20 mmol P m^{-3} and MAE of 0.18 mmol P m^{-3} in the yearly average DIP concentrations (see Table 5). For the unassimilated data in P1, the calibrated solution gives RMSE and MAE values of 1.53 mmol N m^{-3} and 1.26 mmol N m^{-3} for the average annual DIN concentrations, and mean percentage error (MPE) of 17.5 % in P-uptake.

We validated the optimized solution with the observations (unassimilated) from P2. The change in RMSEs and MAEs, compared to P1, is small. For the annual PP, we obtain RMSE and MAE of 9.50 gC m^{-3} and 6.20 gC m^{-3} (Table 6). Likewise for annual DIP, DIN, and DO, the RMSEs and MAEs are: 0.25 mmol P m^{-3} and 0.20 mmol P m^{-3}, 3.80 mmol N m^{-3} and 3.10 mmol N m^{-3}, and 22.30 mmol O_2 m^{-3} and 21.51 mmol O_2 m^{-3}. Furthermore, the model yields RMSE, MAE, and mean percentage error of 231 tons year^{-1}, 167 tons year^{-1}, and 11.8 % for P-uptake in P2. As there is no significant increase in RMSEs and MAEs, the model is robust in reproducing observations from P2 and passes the validation test.

3.2 Comparison of model results and observations

The model successfully reproduces the observed patterns in the annual and seasonal DIP concentrations for P1 (Fig. 1). The seasonal trends in DIP concentrations between the observations and model also match well, although the latter underestimates the turnover of DIP in 1982 and 1983. Both the model and observations show a drop in the DIP concentrations from year 1986 to 1990, going down to ~1.0 mmol P m^{-3} from ~ 2.0 mmol P m^{-3}. This corresponds to a reduction by 50%. The decline in annual DIP concentrations is even higher, accounting for ~75% reduction, from 1986 to 1990

(Fig. 4, panel H). For the annual DIP, the model underestimates the observations in the initial years of P1. The modelled annual PP fits well to the range and order of magnitude of the observed ones in P1 (Fig. 4, panel A). However, the model predicts an increasing trend in annual integrated PP between 1982 and 1984, whereas the observations show a decrease. The percentage error in the magnitude of the simulated PP is small (∼24%) though. Towards the second half of P1, both the model and observations show a decreasing trend in PP.

Although we did not assimilate DIN and P-uptake observations in the misfit function, the model shows good performance in reproducing their observed trends in P1. Both the model and observations show a linear increase in the average annual DIN concentrations in the productive layer from 1981 to 1990, reaching the maximum of 26 mmol N m^{-3} between the years 1989 and 1990 (Fig. 4, panel F). For every year in P1, the simulated turnover of DIN after winter mixing matches well with the observations (Fig. 1, panel C). However, the model underestimates the seasonal depletion of DIN in the epilimnion. The latter could be because either the predicted nitrogen uptake rates of phytoplankton are low or the model overestimates remineralization. Although the variability between the years in the observed annual P-uptake is higher than the simulated one, the magnitude and trends are comparable between the model and the observations between 1982 and 1990. For most of the years in P1, the annual P-uptake is more than 3500 tons $year^{-1}$.

The ecological model performs reasonably well in reproducing the observations from P2 using the optimized solution from P1. The simulated magnitudes and trends in the seasonal and annual DIP, DIN (Fig 4 panels D, F and Fig 4, panels G, I) and in annual PP and P-uptake (Fig 4, panels E, B) are comparable to the observations. In general, both the model and observations show much lower concentrations of DIP in the epilimnion in P2 than P1 (Fig 1, panels E and F). As far as comparison with observations is concerned, the model underestimates the annual DIP from 2011 to 2014 and overestimates from 2015 to 2019. The reduction in the observed annual DIP from 2011 to 2019 is 44%. However, the model predicts a decrease by only 29% with higher variability between the years. Furthermore, the model overestimates the winter turnover of DIP in the productive layer from 2015 to 2019, though the depletion of DIP in summer is well reproduced throughout the decade. Although the modelled winter DIP concentrations are higher than the observations, these values are well within the range for eu- to mesotrophic systems, such as Lake Geneva.

In contrast to the trend in DIP, the decadal-average DIN concentrations (in the epilimnion) of P1 and P2 are similar (27 mmol N m^{-3} and 29 mmol N m^{-3}). For P2, the model and observations show a slight increase in annual DIN from 2011 to 2019, reaching the maximum value in 2019 at ∼40 mmol N m^{-3} (Fig. 1, panel D). The model captures well the seasonal dynamics in the observed DIN concentrations in the productive layer (Fig. 4, panel B). The patterns in the simulated annual PP fit nicely to the observed one in P2. Moreover, the predicted values and observations for each year are very similar (between 20 and 30 gC m^{-3}). The only exception is the year 2012, where the model underestimates the observed PP. Both the model and observations show a consistent decrease in PP from 2012 onwards. The P-uptake in P2 is reduced by more than a half compared to P1 (Fig. 4, panel E). The observed and simulated P-uptake from 2012 to 2019 show a decreasing trend, although the variability between the years 2013, 2014, and 2015 is higher in the model than observations. The consistent decrease in the observed P-uptake is directly related to reducing DIP concentrations in the productive layer.

3.3 Trophic status and warming scenarios

Table 7 summarizes the results in annual PP for the different combinations of trophic status and warming scenarios. For $H_N L_T$ scenario, which is the P1 simulation, the model yields annual-integrated PP of 440 gC m^{-2}. For the hypothetical scenario, $H_N H_T$, representing high nutrient and high air temperature conditions, we obtain an annual PP of 600 gC m^{-2}. For the low nutrients and high-temperature scenario ($L_N H_T$), which corresponds to the P2 simulation, the model predicts annual PP of 400 gC m^{-2}. And for $L_N L_T$ scenario (also a hypothetical scenario), the simulated PP is 350 gC m^{-2}, which is the lowest of all. Thus, according to the model, warming would have led to an increase in PP by 36% if there was no reduction in nutrient loads since P1. This interpretation is made by comparing $H_N H_T$ & $H_N L_T$ scenarios. Likewise, there would have been an increase in PP by 15%, due to warming, under mesotrophic conditions (comparison of $L_N H_T$ & $L_N L_T$ scenarios). To explore the effects of reduction of nutrient loads on PP, we compare $H_N L_T$ & $L_N L_T$ & $H_N H_T$ & $L_N H_T$ scenarios. If the warming had not occurred, the process of reoligotrophication would have led to a decrease in PP by 21% ($H_N L_T$ and $L_N L_T$ scenarios). And under the present-day warming conditions, the reduction in nutrients would have decreased PP by 33% ($H_N H_T$ & $L_N H_T$ scenarios). According to the model and observations, the decadal-average PP in Lake Geneva has decreased by ∼ 10% from P1 to P2 ($H_N L_T$ & $L_N H_T$)

Tables 8 and 9 list the simulated, annually-averaged, total phytoplankton biomass (PhyC) and remineralization rate (RR) for the five scenarios. The highest PhyC (40.45 mmolC m^{-3}) and RR (2.08 d^{-1}) are predicted for the $H_N H_T$ case, and the lowest PhyC (19.27 mmolC m^{-3}) and RR (0.85 d^{-1}) for the $L_N L_T$ scenario. According to the model, warming contributes to 30% increase in the phytoplankton biomass and in the remineralization rate under eutrophic conditions, where as increases by 10% in PhyC and by 15% in RR in low nutrient conditions. These results are very similar to those for PP.

4 Discussion

4.1 Warming and incomplete reoligotrophication in Lake Geneva

Some of our results are supported by other studies. For example, the model predicts a significant effect of warming on PP (an increase by 36%) under eutrophic conditions ($H_N H_T$ and $H_N L_T$ scenarios, Table 7). This result is consistent with the long-term data analysis of Tadonléké (2010), which indicates a strong impact of warming on the chlorophyll-normalized photosynthesis rates when Lake Geneva was eutrophic. Climate warming is known to stimulate the growth rates of phytoplankton (e.g. cyanobacteria and dinoflagellates as assumed in our model) and also remineralization rates that lead to an increase in PP, particularly when nutrients are not limiting (Yvon-Durocher et al. 2010; De Senerpont Domis et al. 2014). Results of the mesocosm experiments performed by Verbeek et al. (2018) to investigate the interactive effects of warming and reoligotrophication on freshwater phytoplankton are similar to ours. They observed an increase in biomass and PP with warming and later a decrease when nutrients started to decline sharply. In their experiments, algal biomass significantly increased with warming under constant nutrient supply; this corroborates our model's prediction for the $H_N H_T$ scenario.

For both the warming scenarios (under high and low nutrient conditions), the model predicts an increase in PP. It is well reported that rapid and significant warming of the productive layer has happened in lakes worldwide (O'Reilly et al. 2015). The warming of surface waters has been attributed to a rise in air temperature as well as to an increase in solar radiation (Fink et al. 2014). Tadonléké et al. (2009) analysed long-term, in-situ data, from Lake Geneva. Their results revealed that climate warming and higher incident light were important drivers for the increase in PP and chlorophyll *a* with time. Our analysis of shortwave radiation (SWR) data from Lake Geneva revealed that the mean daily radiation has indeed increased by ~10%, particularly for winter and spring seasons, over the last four decades (Fig. 6). To study the effect of SWR per se on PP, we simulated $L_N L_T$ and $H_N L_T$ scenarios with elevated radiation levels (representative of P2). Our results show that the increase in SWR from P1 to P2 corresponds to a small increase in annual PP by 2%. Thus, according to the model, the contribution of increase in SWR to PP is negligible in comparison to that of rise in air temperature.

In reality, PP in Lake Geneva has decreased by ~8-10% from past (P1: 1981-1990) to the present decade (P2: 2011-2019). If we compare this to our four scenarios, it would indicate that the net effect of reduction in nutrients on PP is higher than that of warming. However, 8 to 10% reduction in PP is not significant, considering the decline in DIP concentrations by 60% from P1 to P2. The multi-lake analysis of large hydrochemical data suggests that the temperate lakes can sustain high PP as long as areal phosphorus supply (APS) exceeds 0.54 ± 0.06 g P m^{-2} during the productive season (Müller et al. 2019). In Lake Geneva, APS (0.71 g P m^{-2}) has remained above the threshold until 2014 (Kiefer et al. 2021). Thus, during the initial years of the present decade, the lake was still eutrophic, and then onward started to transition. The latter can also be inferred from the estimates of net ecosystem production (Steinsberger et al. 2021; Fernández Castro et al. 2021). Kiefer et al. (2021) identified the total phosphorus threshold (TP^{sw}_{mix}) for lakes in Switzerland, below which they are classified as mesotrophic systems. They estimated TP^{sw}_{mix} of 20 mg P m^{-3} for Lake Geneva. The average concentration of TP for P2 in Lake Geneva is 21 mg P m^{-3}, which indicates that the lake is not yet, but close to the transition to mesotrophic system.

As the first half and the second half of P2 represents different regime with regards to the lake's trophic status, we performed two further numerical experiments representative of the first half (2011-2014) and the second half (2015-2019) of P2. To account for trophic regime, we forced the model with the 5-year average riverine input load for the first sub-period (2011-2014) and with the other five years' average for the second half. The model predicts the annual average PP of ~530 gC m^{-2} for the first half of P2. This value is close to the one simulated for the hypothetical scenario, $H_N H_T$ (~600 gC m^{-2}). Likewise, the predicted RR for the 2011-2014 period is 1.86 d^{-1}, which is comparable to that of $H_N H_T$ scenario. As the lake was still eutrophic in the first half, it seems there was a positive interactive effect of warming and eutrophication on the growth rates of phytoplankton and RR, resulting to an increase in PP (by 20%) compared to P1. For the second half of P2, the model predicts much lower PP, which is ~300 gC m^{-2}. During the last 2-3 years, TP in Lake Geneva has dropped below 20 mg P m^{-3} (Fig. 1), leading to a significant reduction (by 32% compared to P1) in annual PP.

Thus, the changes in PP in Lake Geneva from P1 to P2, apparently, happened in two steps. Until the first half of this decade, the positive effect of warming on PP was higher than the negative effect of reducing nutrient loads. The above was mainly due to stimulation in the growth rates of phytoplankton and remineralization. If we compare this to the $H_N H_T$ case, it would mimic a warming under eutrophication like situation. However, the latter half of the present decade marks the onset of mesotrophication in Lake Geneva (Fig. 1), and this would be representative of the predicted decrease in PP by ~33% due to reoligotrophication under the present warming conditions ($H_N H_T$ and $L_N H_T$ scenarios). This 'mesotrophication' is also reflected in the decline of P-uptake by phytoplankton from 2013 onwards (Fig. 4). The decline in PP in the last 5 years of P2 is stronger than the increase in PP until the first half of P2. And hence, the net effect is a moderate decrease (by ~ 10%) in the decadal PP from P1 to P2 in Lake Geneva. In contrast, PP in Lake Constance has been significantly reduced largely because the effect of reoligotrophication has completely outweighed the impact of

warming on photosynthesis (Stich and Brinker 2010; Müller et al. 2019). Jeppesen et al. (2005) analysed long-term data from several small and big lakes and observed a general trend of decrease in PP and chlorophyll *a* concentrations with a reduction in nutrient loading. However, they added a caveat that changes in each lake is different from the other, and the effects of climate change are likely to run counter to reoligotrophication.

4.2 Future climate change in Lake Geneva

For the future climate change scenario (RCP8.5), the model predicts that the stratified period will be longer than at present, on an average 250 days in one year, with earlier onsets and later breakups. In particular, the model predicts the warming of the productive layer by at least 3.0°C in the summer months (Fig. 5, Panels A and B), whereas the depth of the winter surface mixed layer would decrease by 50% for the "business-as-usual" warming. The latter results point out a significant reduction in mixing, deep ventilation, and consequently affecting the supply of nutrients for PP (Fig 5, Panels C and D).

Our results are in line with the findings of other climate change studies. The hydrodynamic model of Schwefel et al. (2016) predicts a 50% decrease in events of full mixing in Lake Geneva for the future climate forcing. Woolway and Merchant (2019) simulated changes in mixing regimes of lakes worldwide under RCP6.0 scenario, and their results show a significant reduction in mixing strengths (particularly for temperate lakes) by the end of 21st century. Farrell et al. (2020) applied a coupled physical-biogeochemical model to simulate temperature, nutrients and oxygen dynamics in an oligotrophic lake for different climate change scenarios. For the most extreme case, their model predicted intensified stratification, higher water column stability, and an increase in summer surface water temperature by 3.6°C which is very close to our estimate of ~3.0°C. Likewise, the numerical simulations of future climate show an increase by at least 3.0°C in the top water column of Lake Maggiore and shift from oligomictic to meromictic regime (Fenocchi et al. 2018). Future projections for Lakes Superior, Michigan, Huron, Erie, and Ontario predict a longer duration of thermal stratification and longer periods of nutrient limitation of algal growth (Lehman 2002). Their simulations suggest that the duration of thermal stratification would be ~220 days in most of the Great lakes, comparable to our prediction of 250 days.

According to our model, PP in Lake Geneva would increase by 19% (Table 7), and the ecosystem respiration would increase by 60% under the RCP8.5 scenario (Table 9). Apparently, warming-driven stimulation in growth rates of phytoplankton and in remineralization rate outweighs the effect of low nutrient regeneration (due to reduced winter mixing) on PP. Our results show that the stratified conditions help to confine regenerated nutrients in the euphotic zone, thus supporting PP. Increased nutrient cycling and lake productivity has been suggested as a consequence of a warmer climate (Blenckner et al. 2002). Future climate change is expected to bring back the symptoms of eutrophication, e.g. high PP and biomasses of phytoplankton with slow growth rates and elevated rate of mineralization, in lakes undergoing reoligotrophication (Moss et al. 2011). Future increase in PP have been predicted by other studies as well for the temperate lakes. A modelling study by Markensten et al. (2010) shows an increase in total phytoplankton biomass and PP for a Swedish lake under a future climate scenario. Autotrophic production and the concentration of toxic cyanobacteria in Danish lakes are expected to increase for an extreme future climate case (Trolle et al. 2015). Likewise, significant increases in chlorophyll *a* concentrations have been simulated for different warming conditions in Lake Constance (Peeters et al. 2007). However, our predictions about future PP are contradictory to those of Lehman (2002), and Brooks and Zastrow (2002), as their analyses show decreases in phytoplankton biomasses and chlorophyll *a* concentrations in Great Lakes with climate change. Although our analysis also shows a significant reduction in the future deep mixing, there would still be periods of winter turnover that would supply nutrients to the productive layer from the metalimnion and sustain PP in Lake Geneva. The temperature-dependent algae (e.g. dinoflagellates and cyanobacteria in our model) would constitute a significant part of PP in the future. Indeed, the model suggests that the summer biomass of dinoflagellates and cyanobacteria would increase by 50% by 2085 (Fig. 7). On the contrary, the diatom biomass would decrease by 85%. Several studies point to increases in abundances of temperature-dependent autotrophs in lakes under the predicted future climate (Wagner and Adrian 2009; Elliott 2012; Paerl and Paul 2012; Kosten et al. 2012). Evidently, the eco-physiological traits, such as buoyancy regulation, mixotrophy, low-light and high-temperature tolerance, grazing defence, deep-living and ability to harvest nutrients efficiently, favour functional groups like flagellates and blue-green algae to dominate over other phytoplankton as lakes are warming (Walsby and Schanz 2002; Carey et al. 2012; O'Neil et al. 2012; Walsby and Schanz 2002; Ostrovsky et al. 2013; Salmaso et al. 2018; Wilken et al. 2018).

4.3 Model and observation biases

The uncertainties in the model parameter estimates originate from the structural deficiency in the model (in terms of missing processes) and from the uncertainty in the observations. In this section we discuss these biases. The model systematically overestimates the water temperature in the summer months, particularly during P2 (Figs. 1A and 1B). It is known that the River Rhône intrudes between 15 to 20 m in Lake Geneva and flows as a gravity-driven density current (Fernández Castro et al. 2021). During summer, the river water temperature is lower than that of the lake epilimnion,

and also the river discharge is higher. Thus, along the river plume in the epilimnion, there is a cooling effect during the stratified season in Lake Geneva. Our model does not resolve this local cooling phenomenon due to river intrusion, and hence could overestimate the water temperature in the top 20 m in summer.

The observed and simulated annual PP do not follow the same pattern during P1 (Fig. 4). The observations show a decline in PP from 1982 to 1985, whereas the model suggests an increasing trend. During P1, the lake was highly eutrophic, and nutrients were not limiting. Therefore, changes in annual PP were perhaps driven by top-down controls, e.g. grazing pressure. Heterotrophic and phagotrophic ciliates grow at rates comparable to autotrophic phytoplankton and hence can graze upon them, leading to a decline in PP simultaneously. Results of in-situ experiments by Weisse (1988) show that ciliates and heterotrophic flagellates are the major consumers of autotrophic picoplankton and variations in their grazing rates controlled the spring PP in eutrophic Lake Constance. Our model does not resolve the dynamics of heterotrophic flagellates. In addition, we do not assimilate the zooplankton biomass and grazing rates data in the misfit function, as they are not available for Lake Geneva. And hence, the grazing parameter could not be constrained, which may introduce uncertainty in the simulated grazing control on PP.

In general, the model underestimates the observed uptake of DIN (Figs. 1C and 1D). A possible reason for this could be that the model assumes a constant P:N ratio to simulate DIN and DIP dynamics and does not account for the temporal variations in cellular and seston stoichiometry. It has been suggested that the predictive capability of ecological models might be improved by considering variable stoichiometry of biomass and nutrient uptake (Flynn 2010; Smith et al. 2014; Vinçon-Leite and Casenave 2019). Furthermore, some of the variability in DIP and DIN between the years (particularly during P2) is not well captured by the model. As we do not consider the temporal variations in riverine DIN and DIP fluxes and rather assume decadal-average values representing P1 and P2, the model is less sensitive in reproducing the observed changes between the years in DIN and DIP dynamics. For example, exceptional precipitation events in 2013 triggered high surface runoff of DIN fluxes to the lake and hence high annual DIN concentration (CIPEL report, 2013). However, this deviation from the average DIN flux estimate for P2 is not accounted for in the model—leading to underestimation. Krishna et al. (2021) stressed that it is important to consider the temporal changes in riverine fluxes in the model to simulate seasonal nutrient dynamics accurately. The observations presented in this study are the instantaneous profiles containing signatures of three-dimensional processes, such as river intrusion (Cotte and Vennemann 2020), internal waves and lateral buoyancy-driven flows (Fernández Castro et al. 2021; Doda et al. 2022), that a 1D model does not capture (Ulloa et al. 2019, 2022). The latter may also contributes to discrepancies between the observed and simulated nutrient, PP and temperature dynamics on monthly resolution.

5 Conclusion

This study provides insights on the drivers of primary production (PP) in lakes undergoing reoligotrophication, as global warming continues. Furthermore, we demonstrate the robustness of the coupled model (GOTM-ERGOM) to analyse and interpret observations and its utility to disentangle and quantify the effects of reoligotrophication and climate change on PP. The study's pertinence is enhanced by the availability of a complete long-term monitoring dataset for Lake Geneva. Our results show a marginally decrease in PP ($\sim$ 10%) from the past period (1981 to 1990) to the present period (2011 to 2019). However, until the first half of the decade of 2020, the lake was Eutrophic and PP was positive affected by climate change (including an increase in solar radiation). Towards the second half of the present period, the lake started the transition to a mesotrophic state, resulting in a significant reduction in PP there on. The simulations for the future climate change scenario show that the winter mixing strength in the lake will significantly reduce (almost by 50%) by the end of 21st century. However, the autotrophic production is expected to increase by ~20%. Furthermore, in spite the uncertainty in l_{da} parameter, the optimized solution predicts a reduction in the ecosystem respiration by ~60% in future in Lake Geneva. This indicates that the positive effect of warming on phytoplankton growth and remineralization rates is larger than the effect of reduced mixing strength. Thus, our results suggest that future climate change may bring back the symptoms of eutrophication in large temperate lakes.

Tables

State variable	P1	P2
Dissolved inorganic phosphorous (DIP)	2.0 mmol P m^{-3}	0.5 mmol P m^{-3}
Dissolved inorganic nitrogen (DIN)	40 mmol N m^{-3}	35 mmol N m^{-3}
Initial concentration of Diatoms (iniPP)	10^{-3} mmol N^{-3}	10^{-3} mmol N^{-3}
Initial concentration of Flagellates (iniFF)	10^{-3} mmol N^{-3}	10^{-3} mmol N^{-3}
Initial concentration of Zooplankton (ZooN)	10^{-3} mmol N^{-3}	10^{-3} mmol N^{-3}
Initial concentration of Detritus (DetN)	10^{-3} mmol N^{-3}	10^{-3} mmol N^{-3}

Table 1: Initial values for state variables in ERGOM for the periods P1 (1981-1990) and P2 (2011-2019).

Parameter	Description	Unit	Value
α_1	Half-saturation constant for DIN uptake by diatoms	mmol N m^{-3}	0.40
α_2	Half-saturation constant for DIN uptake by dinoflagellates	mmol N m^{-3}	0.30
α_3	Half-saturation constant for DIN uptake by cyanobacteria	mmol N m^{-3}	0.30
Yc_{dia}	Carbon to Chlorophyll *a* ratio of diatoms	μmol mg^{-1}	6.25
Yc_{flag}	Carbon to Chlorophyll *a* ratio of dinoflagellates	μmol mg^{-1}	6.25
Yc_{cya}	Carbon to Chlorophyll *a* ratio of cyanobacteria	μmol mg^{-1}	6.25
rfc	Redfield C to N ratio	mmol C (mmol N)$^{-1}$	6.625
k_c	Light attenuation due to phytoplankton	m^2 mmol C $^{-1}$	0.03
$cyanotll$	Cyanobacteria lower temperature limit	°C	13.5
$cyanosll$	Cyanobacteria lower salinity limit	PSU	1.0
$cyanosul$	Cyanobacteria upper salinity limit	PSU	10.0
$flagtll$	Dinoflagellates temperature dependency	(°C)^2	100.0
T_{opt}	Optimum temperature for zooplankton	°C	20.00
wpz	Diatom sinking rate	m d^{-1}	-0.5
wfz	Dinoflagellates sinking rate	m d^{-1}	0.0
wbz	Cyanobacteria sinking rate	m d^{-1}	0.1
wdz	Detritus sinking rate	m d^{-1}	-4.5
nb	Phytoplankton excretion rate	d^{-1}	0.01
δ	Phytoplankton mortality rate	d^{-1}	0.02
ν	Zooplankton respiration rate	m^3 mmol N^{-1} d^{-1}	0.01
σ	Zooplankton mortality rate	m^3 mmol N^{-1} d^{-1}	0.03
l_{sa}	Sediment mineralization rate	d^{-1}	0.002
$q10_{rec}$	Sediment recycling q10 rule factor	–	0.15
ade_{r0}	Chemoautolithotrophic denitrification rate	d^{-1}	0.1
α_{ade}	Half-saturation constant for chemoautolithotrophic denitrification	mmol N m^{-3}	1.0
$sedrate$	Detritus sedimentation rate	m d^{-1}	2.25
$po4ret$	Phosphate retention fraction, oxic sediments	-	0.18
$pburialrate$	Phosphate burial fraction	-	0.007
$sburialrate$	Sediment burial fraction	-	0.001
$pliberationrate$	Phosphate liberation fraction, anoxic sediments	-	0.1
$br0$	Bioresuspension rate	d^{-1}	0.1
$pvel$	Piston velocity	m d^{-1}	5.0

Table 2: Fixed ERGOM parameters.

Parameter	Description	1981-1990 (P1)	2011-2019 (P2)	Unit
sfl_{po}	Surface phosphate flux	0.10	0.03	mmol P m^{-2} d^{-1}
sfl_{nn}	Surface nitrate flux	0.6	0.4	mmol N m^{-2} d^{-1}
rfr	P to N ratio of seston	0.05	0.03	mmol P (mmol N)$^{-1}$

Table 3: Period specific parameters.

Parameter	Description	optimized value	Uncertainty (standard deviation)	Unit
r_1^{max}	Maximum potential growth rate of diatoms	1.30	± 0.14	d^{-1}
r_2^{max}	Maximum potential growth rate of dinoflagellates	0.90	± 0.05	d^{-1}
r_3^{max}	Maximum potential growth rate of cyanobacteria	0.40	± 0.02	d^{-1}
g_{max}	Maximum grazing rate	0.31	± 0.09	d^{-1}
l_{da}	Detritus remineralization rate	0.03	± 0.03	d^{-1}

Table 4: Optimized model parameters for P1 and validated against P2.

Assimilated variable	**RMSE**	**MAE**
PP (annual-integrated, depth-averaged)	6.70 gC m^{-3}	6.10 gC m^{-3}
DIP (annual-average)	0.20 mmol P m^{-3}	0.18 mmol P m^{-3}
Unassimilated variable		
Temp	0.7°C	0.4°C
DIN	1.53 mmol N m^{-3}	1.26 mmol N m^{-3}
P-uptake	760 tons $year^{-1}$	625 tons $year^{-1}$

Table 5: Root mean square errors (RMSEs) and mean absolute errors (MAEs) in the assimilated and unassimilated variables corresponding to the optimized solution for P1.

Variable	**RMSE**	**MAE**
PP	9.50 gC m^{-3}	6.20 gC m^{-3}
DIP	0.25 mmol P m^{-3}	0.20 mmol P m^{-3}
Temp	0.61°C	0.35°C
DIN	3.80 mmol N m^{-3}	3.10 mmol N m^{-3}
P-uptake	231 tons $year^{-1}$	167 tons $year^{-1}$
DO	22.30 mmol O_2 m^{-3}	21.51 mmol O_2 m^{-3}

Table 6: Root mean square errors (RMSEs) and mean absolute errors (MAEs) corresponding to validation of the model solution with observed variables from P2.

Scenario	**Annual primary production**
$H_N H_T$	600 gC m^{-2}
$H_N L_T$ (P1 simulation)	440 gC m^{-2}
$L_N H_T$ (P2 simulation)	400 gC m^{-2}
$L_N L_T$	350 gC m^{-2}
$L_N H_T$ solution with RCP 8.5	476 gC m^{-2}

Table 7: Annual primary production corresponding to the four scenarios. $H_N L_T$ represents P1 simulation whereas $L_N H_T$ is the simulation for the present (2011-2019) decade.

Scenario	**Total phytoplankton biomass**
$H_N H_T$	40.5 mmolC m^{-3}
$H_N L_T$ (P1 simulation)	31.2 mmolC m^{-3}
$L_N H_T$ (P2 simulation)	21.2 mmolC m^{-3}
$L_N L_T$	19.3 mmolC m^{-3}
$L_N H_T$ solution with RCP 8.5	25.3 mmolC m^{-3}

Table 8: Annually-averaged total phytoplankton biomass (averaged over top 20 m) corresponding to the four scenarios. $H_N L_T$ represents P1 simulation whereas $L_N H_T$ is the simulation for the present (2011-2019) decade.

Scenario	**Remineralization rates**
$H_N H_T$	2.08 d^{-1}
$H_N L_T$ (P1 simulation)	1.60 d^{-1}
$L_N H_T$ (P2 simulation)	1.00 d^{-1}
$L_N L_T$	0.85 d^{-1}
$L_N H_T$ solution with RCP 8.5	1.53 d^{-1}

Table 9: Annually-averaged remineralization rates (averaged over top 20 m) corresponding to the four scenarios. $H_N L_T$ represents P1 simulation whereas $L_N H_T$ is the simulation for the present (2011-2019) decade.

Figures

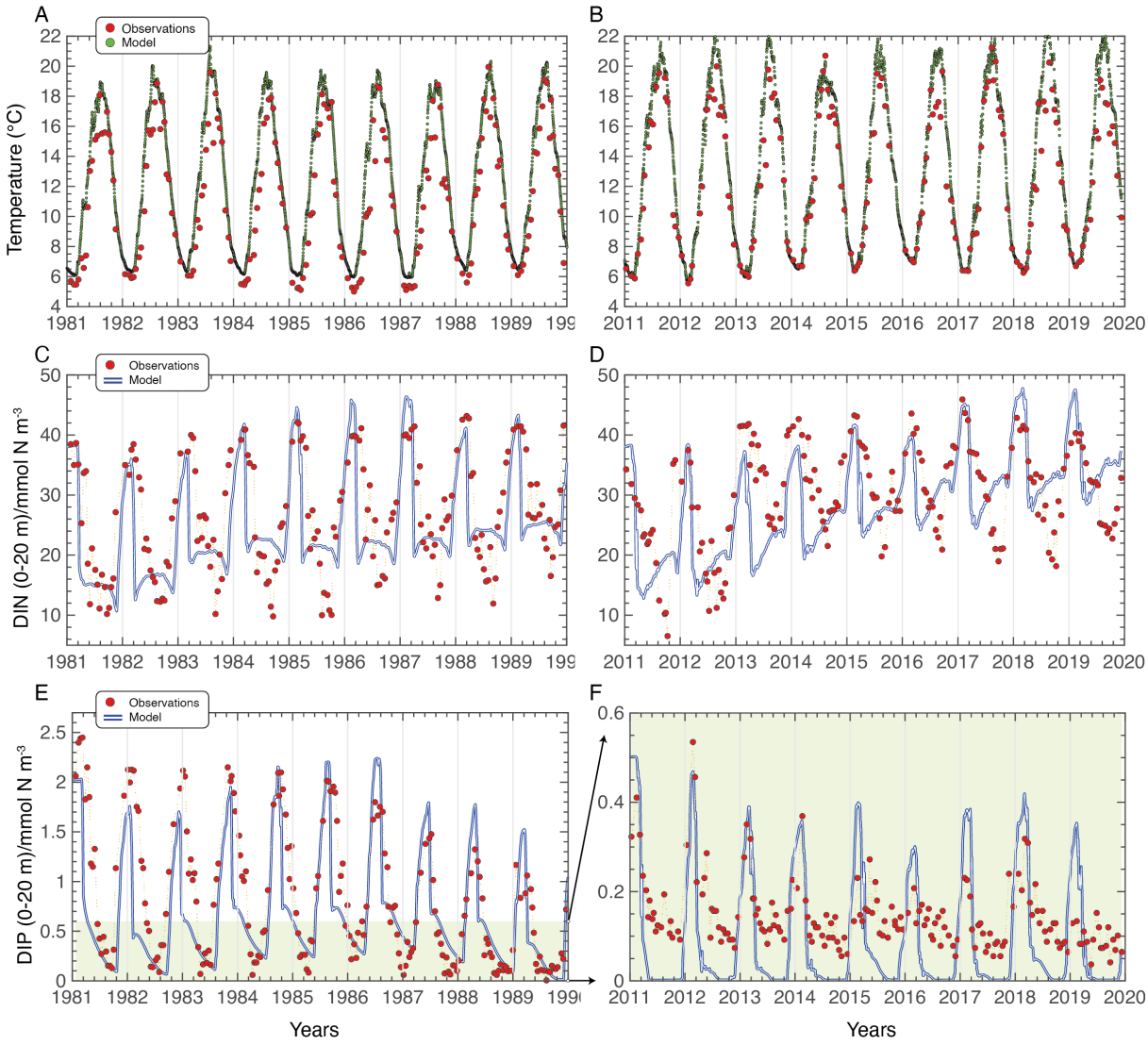

Fig. 1: Observed and simulated Temperature (Panel A), DIN (Panel C) and DIP (Panel E), from the top 20 m, for the past period. Whereas Panels B,D and F show the same for the present period. Note the change of scale for DIP from P1 to P2 (Panel E to F). The observations (red points) are shown at monthly resolution and the model results (solid lines) are shown at daily resolution.

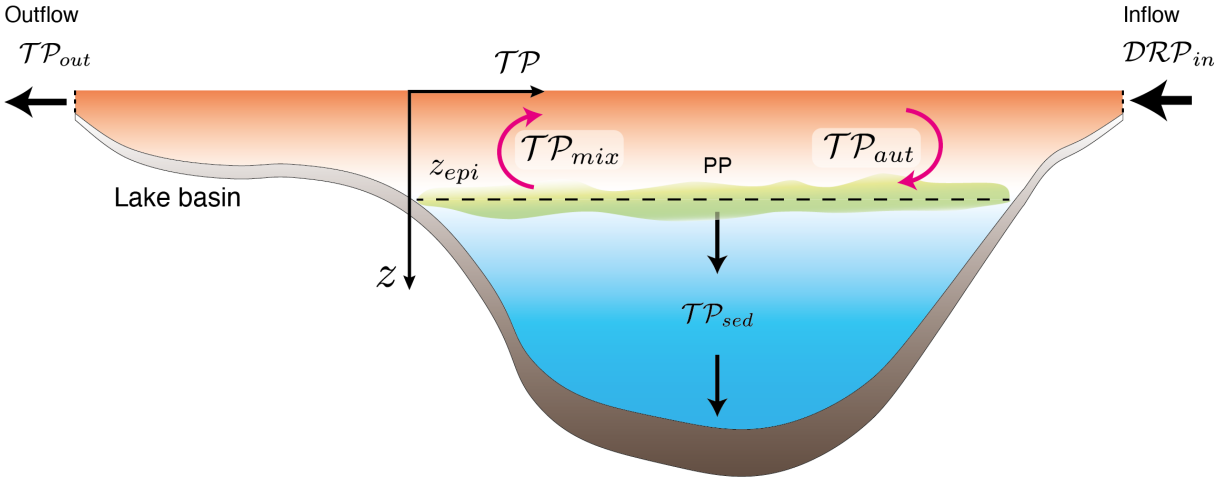

Fig. 2: Schematic of phosphorus budget in Lake Geneva. Dashed line represents the productive layer depth. $[TP]_{mix}$ is the TP load in the productive layer, after winter mixing, in March and $[TP]_{aut}$ is the TP load left after the productive period in October. $[TP]_{sed}$ is the annual TP load that goes into lake sediment. $[TP]_{out}$ is the annual outflow of the riverine TP load and $[DRP]_{in}$ is the annual inflow of the total bioavailable P load.

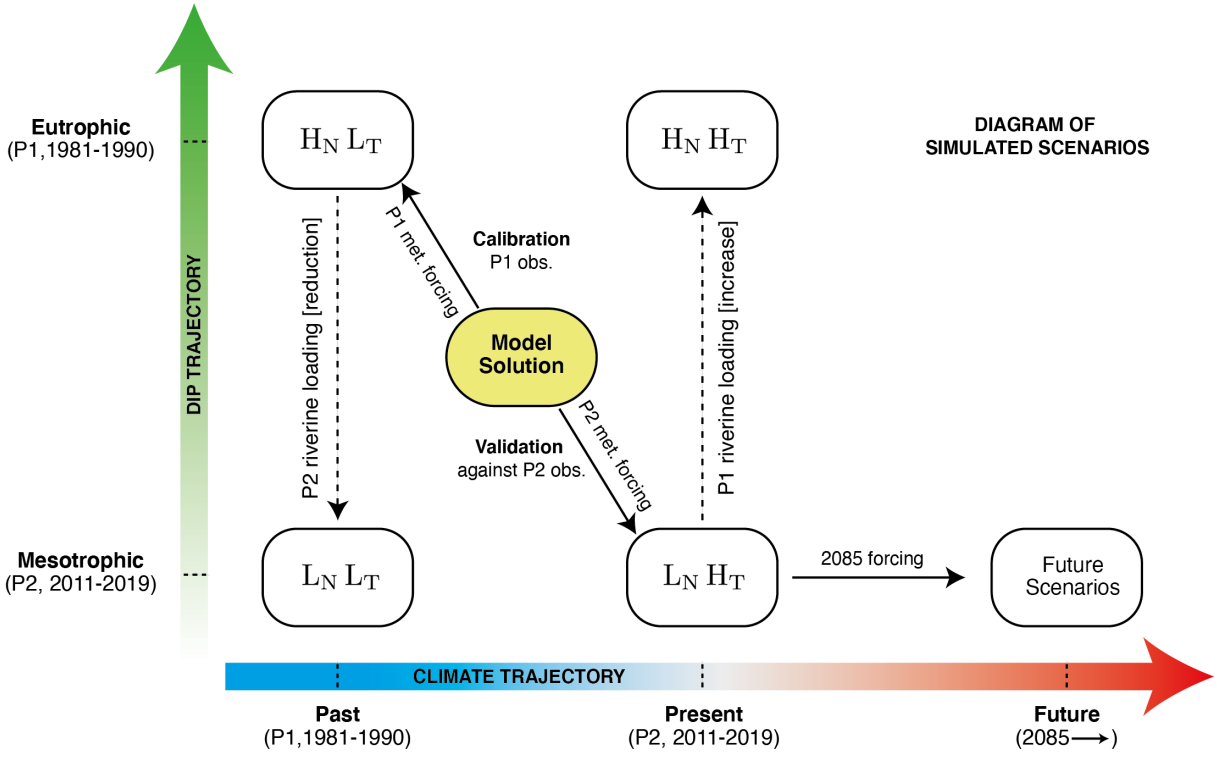

Fig. 3: Schematics of the five simulated scenarios of warming and trophic state. $H_N L_T$ simulation represents the high nutrients and low temperature conditions, mimicking the past period (P1). $L_N H_T$ is the present period (P2) scenario, low nutrients and high temperature. $H_N H_T$ and $L_N L_T$ are the two hypothetical cases simulating the high temperature & high nutrient and the low temperature & low nutrients conditions.

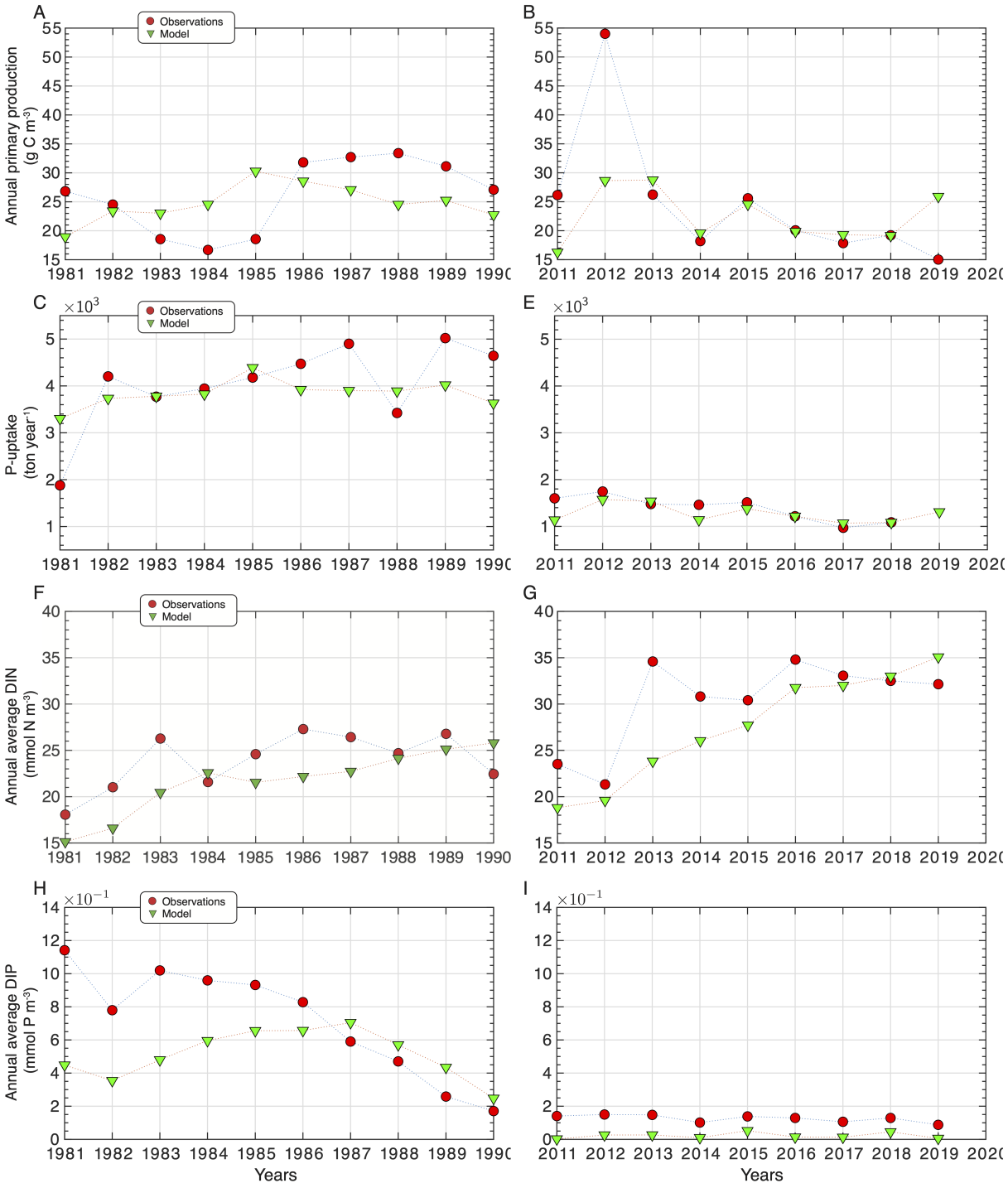

Fig. 4: The observed and simulated annual PP (Panel A), P-uptake (Panel C), DIN (Panel F) and DIP (Panel H), from the top 20 m, for the past period. Whereas Panels B,E,G and I show the same for the present period.

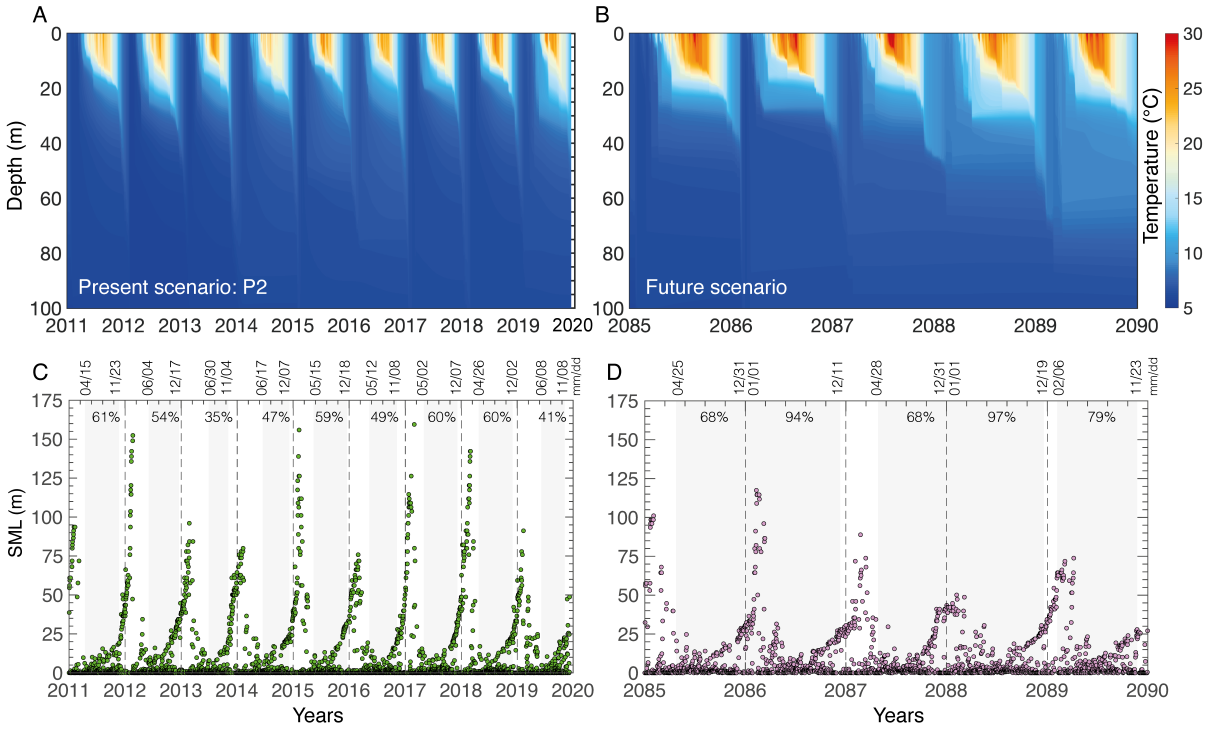

Fig. 5: Panels A and B show simulated temperature profiles for the present period (2011-2020) and for the future years from 2085 to 2090. Whereas Panels C and D show simulated surface mixed layer depth for the present and future periods. Shaded area represents the stratified period and the percentage over the year. Dashed lines denote January 1st of each year. The dates (mm/dd) on top of each year show the time of the onset and breakdown of the annual stratification.

Appendix

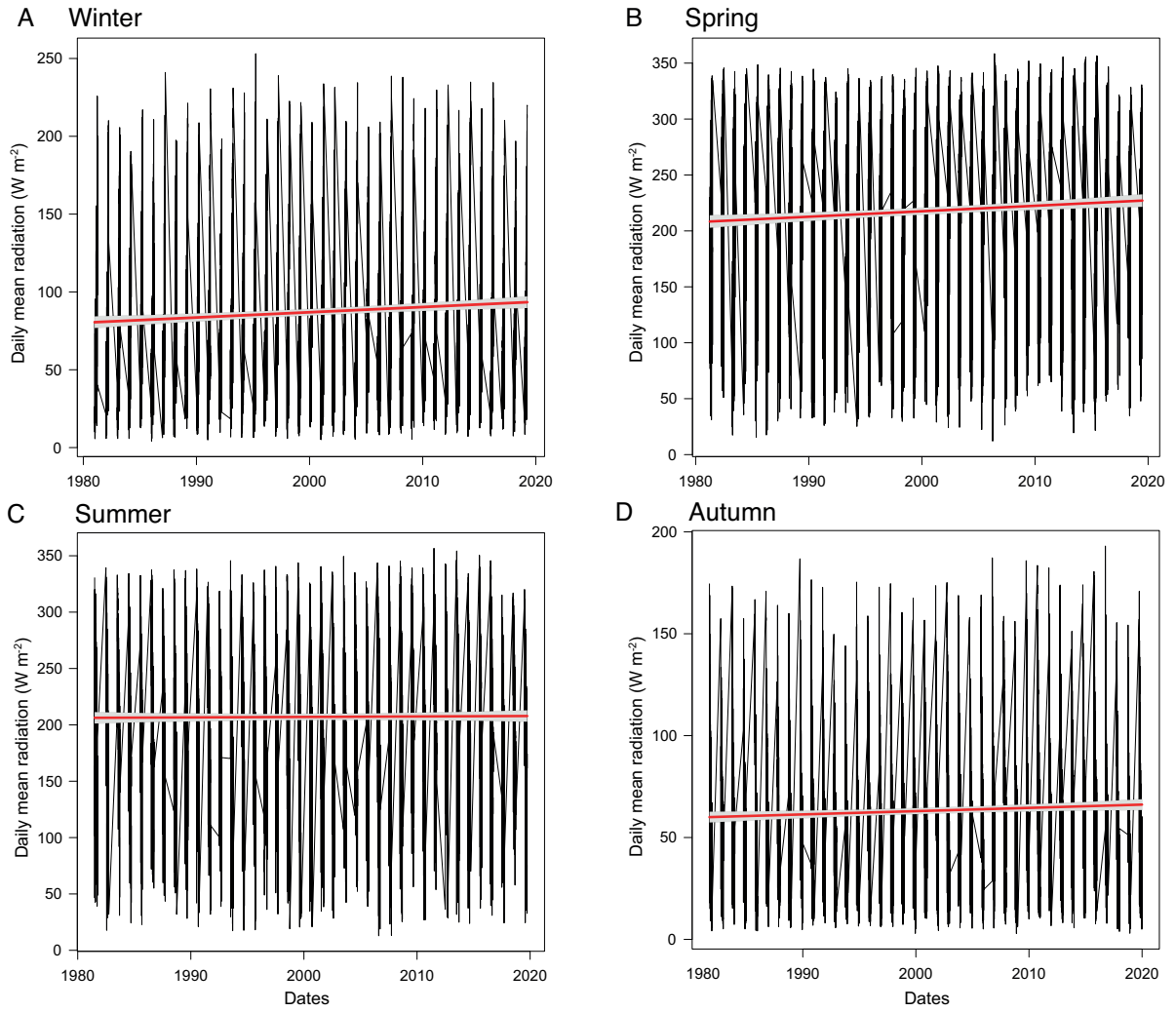

Fig. 6: The long-term changes in the daily mean shortwave radiations for (A) winter, (B) spring, (C) summer and (D) autumn seasons. The blue line denotes the trend.

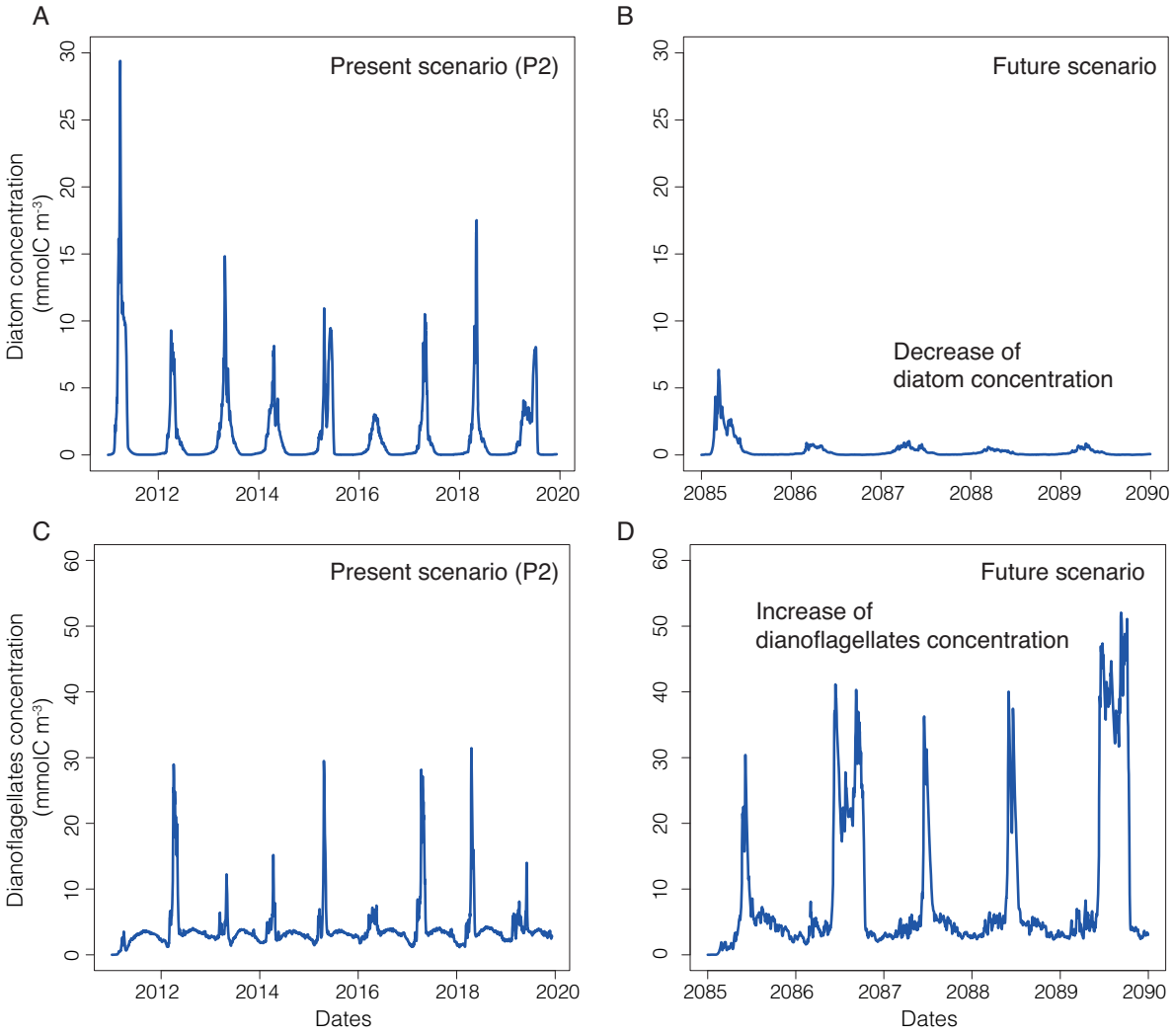

Fig. 7: The simulated diatom and dinoflagellate concentrations for P2(2011-2020) and for the future years 2085 to 2090.

Acknowledgements We are thankful to all member of Aquatic Physics Laboratory (APHYS) at EPFL for their suggestions during the study.

Data Availability Statement

The observations analysed in this study are available at https://si-ola.inrae.fr. The model data is available on request to the corresponding author.

Conflict of interest

We have no conflict of interest with anyone.

References

Adrian R, O'Reilly CM, Zagarese H, Baines SB, Hessen DO, Keller W, Livingstone DM, Sommaruga R, Straile D, Van Donk E, et al. (2009) Lakes as sentinels of climate change. Limnology and Oceanography 54(6part2):2283–2297

Anderson NJ, Jeppesen E, Søndergaard M (2005) Ecological effects of reduced nutrient loading (oligotrophication) on lakes: An introduction. Freshwater Biol 50(10):1589–1593

Anderson NJ, Bennion H, Lotter AF (2014) Lake eutrophication and its implications for organic carbon sequestration in Europe. Global Change Biology 20(9):2741–2751

Anneville O, Chang CW, Dur G, Souissi S, Rimet F, Hao Hsieh C (2019) The paradox of re-oligotrophication: the role of bottom–up versus top–down controls on the phytoplankton community. Oikos 128:1666–1677

Baldauf M, Seifert A, Förstner J, Majewski D, Raschendorfer M, Reinhardt T (2011) Operational convective-scale numerical weather prediction with the Cosmo model: Description and sensitivities. Monthly Weather Review 139(12):3887–3905

Blenckner T, Omstedt A, Rummukainen M (2002) A Swedish case study of contemporary and possible future consequences of climate change on lake function. Aquatic Sciences 64(2):171–184

Brooks AS, Zastrow JC (2002) The potential influence of climate change on offshore primary production in Lake Michigan. J Great Lakes Res 28(4):597–607

Bruggeman J, Bolding K (2014) A general framework for aquatic biogeochemical models. Environ Modell Softw 61:249–265

Burchard H, Bolding K, Kühn W, Meister A, Neumann T, Umlauf L (2006) Description of a flexible and extendable physical-biogeochemical model system for the water column. J Marine Syst 61(3-4):180–211

Carey CC, Ibelings BW, Hoffmann EP, Hamilton DP, Brookes JD (2012) Eco-physiological adaptations that favour freshwater cyanobacteria in a changing climate. Water Res 46(5):1394–1407

Carpenter SR, Ludwig D, Brock WA (1999) Management of eutrophication for lakes subject to potentially irreversible change. Ecol Appl 9(3):751–771

Chen W, Nielsen A, Andersen TK, Hu F, Chou Q, Søndergaard M, Jeppesen E, Trolle D (2019) Modeling the ecological response of a temporarily summer-stratified lake to extreme heatwaves. Water 12(1):94

Cotte G, Vennemann TW (2020) Mixing of Rhône River water in Lake Geneva: Seasonal tracing using stable isotope composition of water. J Great Lakes Res 46(4):839–849, DOI 10.1016/j.jglr.2020.05.015

Darko D, Trolle D, Asmah R, Bolding K, Adjei KA, Odai SN (2019) Modeling the impacts of climate change on the thermal and oxygen dynamics of Lake Volta. J Great Lakes Res 45(1):73–86

De Senerpont Domis LN, Van de Waal DB, Helmsing NR, Van Donk E, Mooij WM (2014) Community stoichiometry in a changing world: combined effects of warming and eutrophication on phytoplankton dynamics. Ecology 95(6):1485–1495

Dennis Jr JE, Schnabel RB (1996) Numerical methods for unconstrained optimization and nonlinear equations. SIAM

Doda T, Ramón CL, Ulloa HN, Wüest A, Bouffard D (2022) Seasonality of density currents induced by differential cooling. Hydrol Earth Syst Sc 26(2):331–353, DOI 10.5194/hess-26-331-2022

Edmondson WT, Lehman JT (1981) The effect of changes in the nutrient income on the condition of Lake Washington. Limnol Oceanogr 26(1):1–29

Elliott JA (2012) Is the future blue-green? A review of the current model predictions of how climate change could affect pelagic freshwater cyanobacteria. Water Res 46(5):1364–1371

Elliott JA, Jones ID, Thackeray SJ (2006) Testing the sensitivity of phytoplankton communities to changes in water temperature and nutrient load, in a temperate lake. Hydrobiologia 559(1):401–411

Farrell KJ, Ward NK, Krinos AI, Hanson PC, Daneshmand V, Figueiredo RJ, Carey CC (2020) Ecosystem-scale nutrient cycling responses to increasing air temperatures vary with lake trophic state. Ecol Model 430:109134

Fenocchi A, Rogora M, Sibilla S, Ciampittiello M, Dresti C (2018) Forecasting the evolution in the mixing regime of a deep subalpine lake under climate change scenarios through numerical modelling (Lake Maggiore, Northern Italy/Southern Switzerland). Clim Dynam 51(9-10):3521–3536

Fernández Castro B, Bouffard D, Troy C, Ulloa HN, Piccolroaz S, Sepúlveda Steiner O, Chmiel HE, Serra Moncadas L, Lavanchy S, Wüest A (2021) Seasonality modulates wind-driven mixing pathways in a large lake. Communications Earth & Environment 2(1):215, DOI 10.1038/s43247-021-00288-3

Fernández Castro B, Chmiel HE, Minaudo C, Krishna S, Perolo P, Rasconi S, Wüest A (2021) Primary and net ecosystem production in a large lake diagnosed from high-resolution oxygen measurements. Water Resources Research 57(2), DOI 10.1029/2020WR029283

Finger D, Wüest A, Bossard P (2013) Effects of oligotrophication on primary production in peri-alpine lakes. Water Resour Res 49(8):4700–4710

Fink G, Schmid M, Wahl B, Wolf T, Wüest A (2014) Heat flux modifications related to climate-induced warming of large European lakes. Water Resources Research 50(3):2072 – 2085, DOI 10.1002/2013WR014448

Flynn KJ (2010) Ecological modelling in a sea of variable stoichiometry: dysfunctionality and the legacy of Redfield and Monod. Progress in Oceanography 84(1-2):52–65

Forsberg C, Ryding S (1980) Eutrophication parameters and trophic state indices in 30 Swedish waste-receiving lakes. Arch Hydrobiol 89:189–207

Gray E, Elliott JA, Mackay EB, Folkard AM, Keenan PO, Jones ID (2019) Modelling lake cyanobacterial blooms: Disentangling the climate-driven impacts of changing mixed depth and water temperature. Freshwater Biol 64(12):2141–2155

Hecky R (1993) The eutrophication of Lake Victoria. Verh lnternat Verein Limnol 25(1):39–48
IPCC (2014) Climate Change 2014: Synthesis Report. Contribution of Working Groups I, II and III to the Fifth Assessment Report of the Intergovernmental Panel on Climate Change [Core Writing Team, R.K. Pachauri and L.A. Meyer (eds.)]. IPCC, Geneva, Switzerland, 151 pp.
Jeppesen E, Søndergaard M, Jensen JP, Havens KE, Anneville O, Carvalho L, Coveney MF, Deneke R, Dokulil MT, Foy B, et al. (2005) Lake responses to reduced nutrient loading–an analysis of contemporary long-term data from 35 case studies. Freshwater biology 50(10):1747–1771
Kerimoglu O, Jacquet S, Vinçon-Leite B, Lemaire BJ, Rimet F, Soulignac F, Trévisan D, Anneville O (2017) Modelling the plankton groups of the deep, peri-alpine Lake Bourget. Ecol Model 359:415–433
Kiefer I, Müller B, Wüest A (2021) Anleitung zur Analyse von Sauerstoffzehrung und Netto-Ökosystemproduktion. Eawag and EPFL, https://wwwdoralib4rich/eawag/islandora/object/eawag:21995
Kosten S, Huszar VL, Bécares E, Costa LS, van Donk E, Hansson LA, Jeppesen E, Kruk C, Lacerot G, Mazzeo N, et al. (2012) Warmer climates boost cyanobacterial dominance in shallow lakes. Global Change Biol 18(1):118–126
Krishna S, Ulloa HN, Kerimoglu O, Minaudo C, Anneville O, Wüest A (2021) Model-based data analysis of the effect of winter mixing on primary production in a lake under reoligotrophication. Ecological Modelling 440:109401
Lehman JT (2002) Mixing patterns and plankton biomass of the St. Lawrence Great Lakes under climate change scenarios. J Great Lakes Res 28(4):583–596
Lepori F, Roberts JJ (2015) Past and future warming of a deep European lake (Lake Lugano): What are the climatic drivers? J Great Lakes Res 41(4):973–981
Lepori F, Roberts JJ, Schmidt TS (2018) A paradox of warming in a deep peri-alpine lake (Lake Lugano, Switzerland and Italy). Hydrobiologia 824(1):215–228
Lindim C, Becker A, Grüneberg B, Fischer H (2015) Modelling the effects of nutrient loads reduction and testing the N and P control paradigm in a German shallow lake. Ecol Eng 82:415–427
Markensten H, Moore K, Persson I (2010) Simulated lake phytoplankton composition shifts toward cyanobacteria dominance in a future warmer climate. Ecological Applications 20(3):752–767
Molteni F, Buizza R, Palmer TN, Petroliagis T (1996) The ECMWF ensemble prediction system: Methodology and validation. Quarterly journal of the Royal Meteorological Society 122(529):73–119
Moss B, Kosten S, Meerhoff M, Battarbee R, Jeppesen E, Mazzeo N, Havens K, Lacerot G, Liu Z, De Meester L, Paerl H, Scheffer M (2011) Allied attack: climate change and eutrophication. Inland Waters 1(2):101–105
Müller B, Steinsberger T, Schwefel R, Gächter R, Sturm M, Wüest A (2019) Oxygen consumption in seasonally stratified lakes decreases only below a marginal phosphorus threshold. Scientific Reports 9:18054. https://doi.org/10.1038/s41598–019–54486–3
Neumann T (2000) Towards a 3D-ecosystem model of the Baltic Sea. J Marine Syst 25(3-4):405–419
Neumann T, Fennel W, Kremp C (2002) Experimental simulations with an ecosystem model of the Baltic Sea: A nutrient load reduction experiment. Global Biogeochem Cy 16(3):1033
O'Reilly CM, Alin SR, Plisnier PD, Cohen AS, McKee BA (2003) Climate change decreases aquatic ecosystem productivity of Lake Tanganyika, Africa. Nature 424(6950):766–768
O'Reilly CM, Sharma S, Gray DK, Hampton SE, Read JS, Rowley RJ, Schneider P, Lenters JD, McIntyre PB, Kraemer BM, et al. (2015) Rapid and highly variable warming of lake surface waters around the globe. Geophysical Research Letters 42(24):10–773
Ostrovsky I, Rimmer A, Yacobi YZ, Nishri A, Sukenik A, Hadas O, Zohary T (2013) Long-term changes in the Lake Kinneret ecosystem: the effects of climate change and anthropogenic factors. Climatic change and global warming of inland waters: impacts and mitigation for ecosystems and societies pp 271–293
O'Neil J, Davis T, Burford M, Gobler C (2012) The rise of harmful cyanobacteria blooms: the potential roles of eutrophication and climate change. Harmful Algae 14:313–334
Paerl HW, Paul VJ (2012) Climate change: links to global expansion of harmful cyanobacteria. Water Res 46(5):1349–1363
Peeters F, Straile D, Lorke A, Livingstone DM (2007) Earlier onset of the spring phytoplankton bloom in lakes of the temperate zone in a warmer climate. Global Change Biology 13(9):1898–1909
Reynolds CS (1999) Modelling phytoplankton dynamics and its application to lake management. Hydrobiologia 395:123–131
Rimet F, Anneville O, Barbet D, Chardon C, Crépin L, Domaizon I, Dorioz JM, Espinat L, Frossard V, Guillard J, Goulon C, Hamelet V, Hustache JC, Jacquet S, Lainé L, Montuelle B, Perney P, Quetin P, Rasconi S, Schellenberger A, Tran-Khac V, Monet G (2020) The Observatory on LAkes (OLA) database: Sixty years of environmental data accessible to the public. J Limnol 79(2):164–178
Rinke K, Eder M, Peeters F, Kümmerlin R, Gal G, Rothhaupt KO (2009) Simulating phytoplankton community dynamics in Lake Constance with a coupled hydrodynamic-ecological model. Verh lnternat Verein Limnol 30(5):701–704
Salmaso N, Boscaini A, Capelli C, Cerasino L (2018) Ongoing ecological shifts in a large lake are driven by climate change and eutrophication: evidences from a three-decade study in Lake Garda. Hydrobiologia 824(1):177–195
Schartau M, Oschlies A (2003) Simultaneous data-based optimization of a 1d-ecosystem model at three locations in the north atlantic: Part i—method and parameter estimates. Journal of Marine Research 61(6):765–793
Schartau M, Wallhead P, Hemmings J, Löptien U, Kriest I, Krishna S, Ward BA, Slawig T, Oschlies A (2017) Reviews and syntheses: parameter identification in marine planktonic ecosystem modelling. Biogeosciences 14(6):1647–1701
Schindler D (2009) Lakes as sentinels and integrators for the effects of climate change on watersheds, airsheds, and landscapes. Limnol Oceanogr 54(6, part2):2349–2358
Schindler DW (1997) Widespread effects of climatic warming on freshwater ecosystems in NorthAmerica. Hydrological processes 11(8):1043–1067
Schindler DW, Carpenter SR, Chapra SC, Hecky RE, Orihel DM (2016) Reducing phosphorus to curb lake eutrophication is a success. Environmental Science & Technology 50(17):8923–8929
Schwefel R, Gaudard A, Wüest A, Bouffard D (2016) Effects of climate change on deepwater oxygen and winter mixing in a deep lake (Lake Geneva): Comparing observational findings and modeling. Water Resources Research 52(11):8811–8826
Schwefel R, Müller B, Boisgontier H, Wüest A (2019) Global warming affects nutrient upwelling in deep lakes. Aquatic Sciences 81(3): 50, Doi: 10.1007/s00027-019-0637-0
Smith SL, Merico A, Wirtz KW, Pahlow M (2014) Leaving misleading legacies behind in plankton ecosystem modelling. Journal of Plankton Research 36(3):613–620
Steinsberger T, Wüest A, Müller B (2021) Net ecosystem production of lakes estimated from hypolimnetic organic carbon sinks. Water Resources Research 57(5), DOI 10.1029/2020WR029473
Stich HB, Brinker A (2010) Oligotrophication outweighs effects of global warming in a large, deep, stratified lake ecosystem. Global Change Biol 16(2):877–888

Straile D, Kerimoglu O, Peeters F, Jochimsen MC, Kümmerlin R, Rinke K, Rothhaupt KO (2010) Effects of a half a millennium winter on a deep lake - a shape of things to come? Global Change Biol 16(10):2844–2856
Tadonléké RD (2010) Evidence of warming effects on phytoplankton productivity rates and their dependence on eutrophication status. Limnology and Oceanography 55(3):973–982
Tadonléké RD, Lazzarotto J, Anneville O, Druart JC (2009) Phytoplankton productivity increased in Lake Geneva despite phosphorus loading reduction. Journal of Plankton Research 31(10):1179–1194
Tirok K, Gaedke U (2007) The effect of irradiance, vertical mixing and temperature on spring phytoplankton dynamics under climate change: Long-term observations and model analysis. Oecologia 150(4):625–642
Trolle D, Skovgaard H, Jeppesen E (2008) The Water Framework Directive: Setting the phosphorus loading target for a deep lake in Denmark using the 1D lake ecosystem model DYRESM-CAEDYM. Ecol Model 219(1-2):138–152
Trolle D, Nielsen A, Rolighed J, Thodsen H, Andersen HE, Karlsson IB, Refsgaard JC, Olesen JE, Bolding K, Kronvang B, et al. (2015) Projecting the future ecological state of lakes in Denmark in a 6 degree warming scenario. Climate Research 64(1):55–72
Ulloa HN, Winters KB, Wüest A, Bouffard D (2019) Differential heating drives downslope flows that accelerate mixed-layer warming in ice-covered waters. Geophysical Research Letters 46(23):13872–13882, DOI https://doi.org/10.1029/2019GL085258
Ulloa HN, Ramón CL, Doda T, Wüest A, Bouffard D (2022) Development of overturning circulation in sloping waterbodies due to surface cooling. Journal of Fluid Mechanics 930:A18, DOI https://doi.org/10.1017/jfm.2021.883
Van Donk E, Hessen DO, Verschoor AM, Gulati RD (2008) Re-oligotrophication by phosphorus reduction and effects on seston quality in lakes. Limnologica 38(3-4):189–202
Verbeek L, Gall A, Hillebrand H, Striebel M (2018) Warming and oligotrophication cause shifts in freshwater phytoplankton communities. Global Change Biology 24(10): 4532– 4543, https://doi.org/10.1111/gcb.14337
Vinçon-Leite B, Casenave C (2019) Modelling eutrophication in lake ecosystems: a review. Science of the Total Environment 651:2985–3001
Wagner C, Adrian R (2009) Cyanobacteria dominance: quantifying the effects of climate change. Limnol Oceanogr 54(6, part2):2460–2468
Walsby A, Schanz F (2002) Light-dependent growth rate determines changes in the population of *Planktothrix rubescens* over the annual cycle in Lake Zürich, Switzerland. New Phytologist 154(3):671–687
Ward NK, Steele BG, Weathers KC, Cottingham KL, Ewing HA, Hanson PC, Carey CC (2020) Differential responses of maximum versus median chlorophyll *a* to air temperature and nutrient loads in an oligotrophic lake over 31 years. Water Resources Research 56(7), e2020WR027296, https://doi.org/10.1029/2020WR027296(7)
Weisse T (1988) Dynamics of autotrophic picoplankton in Lake Constance. Journal of Plankton Research 10(6):1179–1188
Wilken S, Soares M, Urrutia-Cordero P, Ratcovich J, Ekvall MK, Van Donk E, Hansson LA (2018) Primary producers or consumers? increasing phytoplankton bacterivory along a gradient of lake warming and browning. Limnology and Oceanography 63(S1):S142–S155
Williamson CE, Saros JE, Vincent WF, Smol JP (2009) Lakes and reservoirs as sentinels, integrators, and regulators of climate change. Limnol Oceanogr 54(6, part2):2273–2282
Wilson HL, Ayala AI, Jones ID, Rolston A, Pierson D, de Eyto E, Grossart HP, Perga ME, Woolway RI, Jennings E (2020) Variability in epilimnion depth estimations in lakes. Hydrology and Earth System Sciences 24(11):5559–5577
Wilson JD, Monteiro FM, Schmidt DN, Ward BA, Ridgwell A (2018) Linking marine plankton ecosystems and climate: a new modeling approach to the warm early Eocene climate. Paleoceanogr Paleocl 33(12):1439–1452
Woolway RI, Merchant CJ (2019) Worldwide alteration of lake mixing regimes in response to climate change. Nat Geosci 12(4):271–276
Woolway RI, Dokulil MT, Marszelewski W, Schmid M, Bouffard D, Merchant CJ (2017) Warming of Central European lakes and their response to the 1980s climate regime shift. Climatic Change 142(3-4):505–520
Yvon-Durocher G, Jones JI, Trimmer M, Woodward G, Montoya JM (2010) Warming alters the metabolic balance of ecosystems. Philosophical Transactions of the Royal Society B: Biological Sciences 365(1549):2117–2126